AKADÉMIAI KIADÓ

Pollack Periodica • An International Journal for Engineering and Information Sciences

19 (2024) 2, 102–109

DOI:
10.1556/606.2023.00952

ORIGINAL RESEARCH PAPER

Enhancing pier local scour prediction in the presence of floating debris

Muhanad Al-Jubouri* and Richard P. Ray

Department of Structural and Geotechnical Engineering, Faculty of Civil Engineering, Széchenyi István University, Győr, Hungary

Received: October 3, 2023 • Revised manuscript received: November 11, 2023 • Accepted: November 16, 2023
Published online: February 20, 2024

ABSTRACT

Local scour poses a grave threat to bridge foundations, potentially causing catastrophic collapses. This study uses FLOW-3D with the Reynolds-Averaged Navier-Stokes model to analyze pier scour and dune formation under bridges. It focuses on submerged debris shapes near the water's surface. Results closely match experiments when specific conditions are met. The study introduces an innovative approach to debris impact assessment. Instead of traditional methods, it proposes a novel equation accounting for debris's effective area and elevation. This enhances reliability by over 20%, improving scour depth assessment in debris-laden scenarios. This advances the understanding of debris's role in local scour, benefiting bridge design and management practices.

KEYWORDS

local scouring, non-cohesive, clearwater, dune formation, debris

1. INTRODUCTION

In civil engineering, bridges serve as vital hydraulic structures facing various challenges and risks. These challenges include localized scouring and hydraulic forces resulting from debris accumulation near bridge foundations. Debris, especially floating debris, exacerbates scouring issues, potentially leading to bridge failures. An illustrative incident in Ohio, where a bridge collapsed due to debris accumulation, underscores the vulnerability of such structures [1]. The severity of accumulated debris around bridge piers varies, significantly accelerating scouring by obstructing water flow. Unfortunately, numerous instances of bridge collapse in the United States have been directly linked to scour [2–4]. Accurately predicting scour depths requires nuanced consideration of debris effects, leading to extensive experimental studies to evaluate these intricacies [5–7].

Researchers employ diverse approaches, including numerical simulations, analytical solutions, and experimental investigations [8–11]. Analytical solutions are favored in scour assessment in bridge scenarios due to their practical utility [12, 13]. However, these solutions have limitations, especially in intricate cases. Traditional scour potential calculations may struggle to predict developments in scour cavities around piers due to the three-dimensional nature of horseshoe vortex formation [14]. This complexity necessitates comprehensive 3D non-hydrostatic simulations, a domain where Computational Fluid Dynamics (CFD) proves indispensable [15, 16]. While CFD models offer distinct advantages, challenges exist, such as the meticulous determination of boundary conditions, reconciling disparities in simulating diverse scour scenarios, and precision concerns [17–19]. Ref. [20] used FLOW-3D and the k-ε Re-Normalization Group (RNG) turbulence model to evaluate debris with triangular and rectangular shapes at bridge piers. Results showed that floating material deepens the scour hole, with rectangular debris causing more scour than triangular debris near buildings.

This study introduces a pioneering approach using an active mesh update mechanism-based CFD modeling technique with the FLOW-3D package. It systematically characterizes complex

*Corresponding author.
E-mail: muhanad.kh.99.oo@gmail.com

flow conditions around bridge piers, utilizing Reynolds-Averaged Navier-Stokes (RANS) modeling, k-ε turbulence modeling, and Large-Eddy Simulation (LES). The major goal of the research is to forecast local scour depth in clear water surrounding a cylindrical pier with impervious debris in different configurations. A thorough examination of user-defined factors is carried out to propose a unique equation for exact scour depth estimation based on a series of experiments, particularly in scenarios including debris. The project seeks to improve the safety and dependability of bridge structures across climatic situations by integrating computational modeling with experimental findings. This project represents a substantial development in the knowledge and management of hydraulic issues in civil engineering, providing vital contributions to educational institutions and the real world.

2. EXPERIMENTAL MODEL

An experimental validation of the numerical model was conducted at the laboratory of Iraq's Ministry of Water Resources-Research and Design Center. The setup included a 12.5-meter-long, 0.3-meter-wide, and 0.55-meter-deep canal with transparent glass sides. An electrical pump with a maximum discharge of Q = 85 liters per second supplied flow to the canal. Sluice gates with two-flow straighteners were used to maintain consistent flow and protect the pump. A sediment recess, 6 m long, 0.2 m deep, and 0.3 m wide, was part of the setup to simulate pier scouring effects. Sand with a D_{50} of 0.9 mm was used. The water depth in the flume was 12 cm, with a velocity of approximately 0.27 meters per second. Circular piers with a 2 cm diameter were employed, and various debris shapes (rectangles, triangular bows, high wedges, low wedges, triangle yield signs, and half-cylinders) were introduced into the flow. The dimensions of these debris shapes were W = 12 cm, L = 6 cm, and T = 3 cm. Figures 1 and 2 illustrate the flume setup and the debris shapes used in the experiments.

3. THE VALIDATION OF THE SIMULATION MODEL

In this simulation study, careful attention was given to the design of pier configurations, ensuring a faithful replication of the experimental model's conditions. Commencing

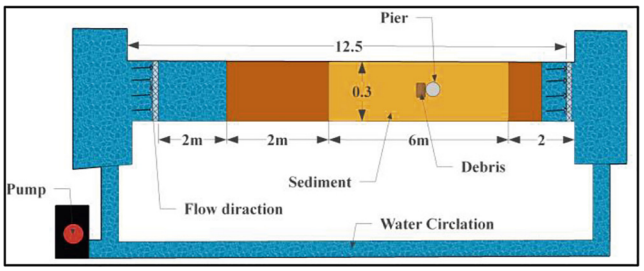

Fig. 1. The flume diagram

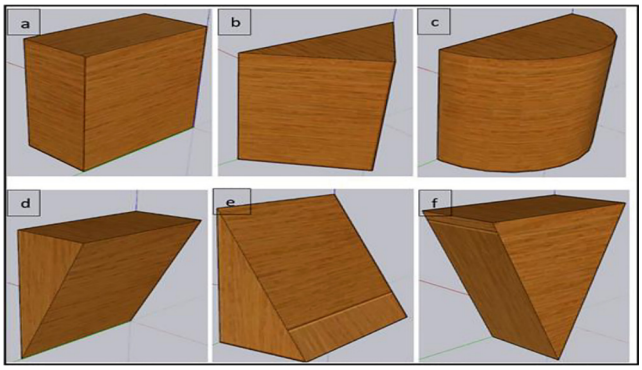

Fig. 2. The simulated debris shape is a) a rectangle; b) a triangle bow; c) a half-cylinder; d) a high wedge; e) a low wedge; and f) a triangle yield sign

the sediment transport simulations involved establishing stable-state hydraulic conditions, providing the foundational framework for subsequent analyses. Activating the sediment model required the utilization of a specific sand particle with a diameter (D50) of 0.93 mm and an average density of 2,650 kg m^{-3}. The computational mesh, featuring a cell size of 6 mm, aimed to faithfully replicate scouring responses consistent with the experimental setup and materials detailed in reference [21]. An important criterion for the simulation was identified: when the flow stream extended twelve times the pier width away from the pier center, the area could be deemed devoid of pier influence. To optimize computational efficiency, the overall dimensions of the computational model were adjusted, with 15 times the pier diameter (15D), 10 times the pier diameter (10D) from the fluid's exit to the pier center location, and 5 times the pier diameter (5D) between the pier center and the entrance side. Consistent with the laboratory experiment, additional variables in the numerical model mirrored those in the physical study. Following the confirmation of agreement percentages between numerical findings and experimental data, critical factors directly impacting results underwent calibration. The calibrated parameter values were subsequently integrated into the computerized simulation. Boundary conditions played a pivotal role in this experiment. The total flow rate (Q) was set at 10 liters per second using the intake, with a standard flow depth of 12 cm. The boundary was specified as a pressure condition with a normal flow depth of 12 cm, the unconstrained terrain represented by Z_{max}, experienced stagnation pressure. Notably, the numerical model's boundary conditions had to align precisely with the physical settings of the study. Key inputs for the model setup included the Nilsen bed-load transfer formula, the RNG standard model with second-order momentum advection, and a surface roughness-to-D50 ratio of 2.5. The FLOW-3D software employed a sophisticated meshing technique known as Flow-3D to efficiently handle complex properties within the computational domain. Fractional Area-Volume Obstacle Representation (FAVOR) ensured numerical stability and accurately determined interface areas, advection, tension, and solid obstacles without relying on a structured grid. The simulation

results underwent meticulous comparison with data from the physical model until a balanced scour depth was achieved. The computational time for each case, spanning 60 min, amounted to approximately 36 h in real-time [17]. In the realm of 3D sediment modeling, a critical challenge lies in establishing accurate relationships for sediment transport. The selection of appropriate transport parameters is a complex task, introducing uncertainty due to the intricate interplay of hydraulic responses and transportation processes, leading to bed height fluctuations during simulations.

4. RESULTS

4.1. Experimental and numerical simulation result

In a comprehensive investigation involving a single pier without debris, the hydraulic flow interaction produced intriguing dynamics. Specifically, it resulted in a vertical pressure gradient along the face of the pier upon impingement. This pressure gradient, in turn, gave rise to a downflow jet, which had the effect of agitating the soil bed and, importantly, inducing the erosion of sand particles. What is worth noting is that a substantial proportion of the bed sediments were entrained by the primary vortex formed around the pier, contributing significantly to the development of the scour hole. As the scouring process unfolded, particles from the scour hole were further entrained in the downstream flow. This was primarily due to the wake vortices generated as the flow divided at the corners of the pier. A key aspect of this investigation was the examination of the impact of various debris shapes on scour depths. Figure 3 provides a visual representation of how different debris shapes influence scour depths, comparing the maximum scour depth in the presence of debris (Y_{sa}) to the baseline condition without debris (Y_s). Each distinct set of vertical bars corresponds to a specific type of debris, while varying shades within the bars are associated with different levels of submersion of the debris, measured from the water-free surface (T = 3, 6, 12 cm), debris length in the upstream direction relative to the pier (L_u = 6, 12 cm), and debris width in the transverse direction (W = 12 cm). What makes this analysis even more intriguing is that it reveals that the

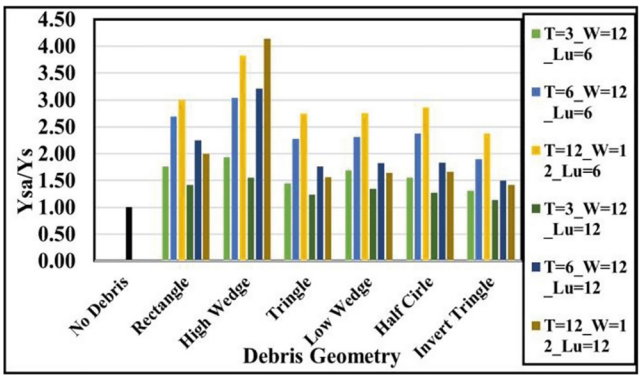

Fig. 3. The relative scour depth (Y_{sa}/Y_s) for all test cases

highest relative scour depths were observed when the debris had high wedge shapes, especially with L_u ranging from 6 to 12 cm and T equal to 12 cm. In all scenarios, the high wedge shape consistently induced significant scouring, making it a crucial factor to consider in bridge design and assessment. Surprisingly, the triangular yield shape resulted in a scour depth comparable to the situation without debris, implying that it was the most detrimental shape in terms of scour generation. The presence of debris at the bridge pier had a profound impact on the scour characteristics and flow patterns in the area. Furthermore, Fig. 4 provides a visual representation of the condition without debris, and it is worth noting that the absence of debris revealed a cleaner flow pattern. Additionally, measurements of debris accumulation are showcased in Fig. 5, highlighting varying scour levels and dune geometries influenced by fluid and morphological factors. These measurements were captured using a surfer program and a camera during the experimental tests offering valuable insights into how debris accumulation affects scour patterns. In summary, this investigation not only sheds light on the complex interactions between hydraulic flow, pier structures, and debris but also provides valuable data for understanding and predicting scour depths in real-world bridge scenarios.

The investigation utilized the FLOW-3D software, conducting a total of seven simulations. The initial simulation focused on an isolated pier scenario, devoid of any debris, while subsequent simulations introduced debris at various depths, specifically positioned 3 cm below the water surface. Figure 6a presents a graphical representation of the temporal evolution of the scour depth observed across these seven simulations. From the results, it becomes evident that the time-dependent scour depth is notably amplified when rectangular debris is present, extending to a depth of 3 cm from the flow surface. Additionally, it is noteworthy that the wedge-shaped debris configurations consistently yield higher scour depths compared to both the scenario without debris and other debris configurations under identical conditions. However, a substantial discrepancy emerges when comparing the numerical simulation outcomes with the data obtained from the physical model, as depicted in Fig. 6b. This disparity is marked by a consistent underestimation of the final scour depth in the software results, with an average deviation of approximately 60% and a Root Mean Square Error (RMSE) value of 3.2, as evidenced in Fig. 7. Several factors contribute to this observed disparity in results. One plausible explanation is the consistent trend observed in previous computerized 3D representations of scour phenomena near piers, which may be attributed to the failure of vortice models to adequately resolve the complex horseshoe vortex system [17]. Additionally, variations in the determination of factors like sediment absorption characteristics, mesh size, sediment equation, surface roughness, shield parameters, and turbulence model selection may also contribute to these discrepancies. It is imperative to underscore the significance of accurately assessing the condition of sand absorption as a response of soil to flow passage, particularly in studies concerning the evaluation of scour holes near

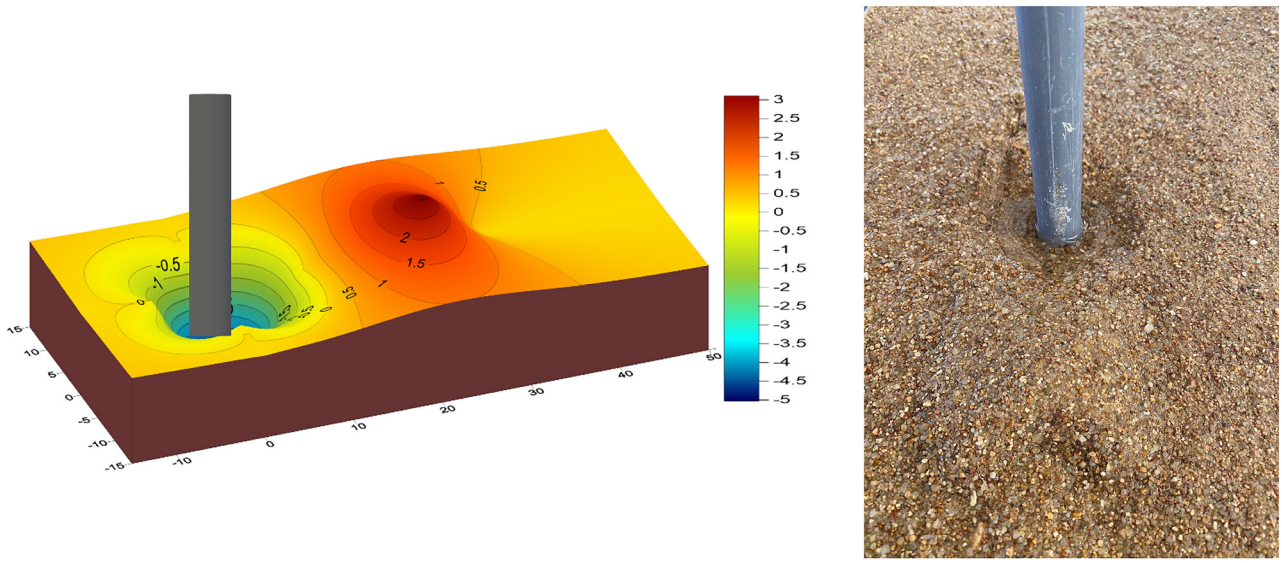

Fig. 4. The behavior of scouring around the bridge pier for no-debris cases in 3D

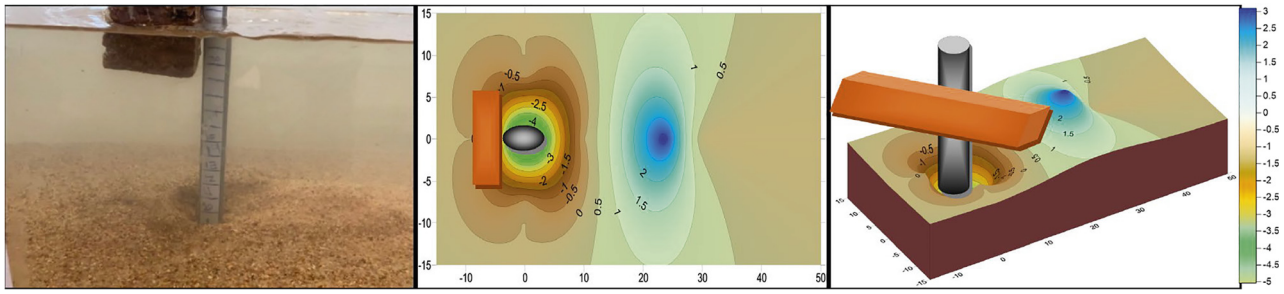

Fig. 5. The maximum scour depth for rectangle debris case at 3 cm below the flow surface in cm

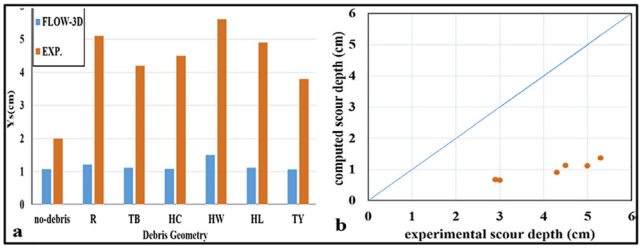

Fig. 6. a) The experimental and numerical scour depth results, b) The estimated vs. the calculated scour depth results

structures and the development of countermeasures. Discrepancies in the assessment of this condition may be a prominent source of variation among the results obtained in numerous acknowledged studies. These differences often stem from the subjective nature of such assessments, which applies equally to numerical analyses. To comprehensively assess the extent to which various input parameters influence simulation outcomes, a factor-testing approach was undertaken in this study. This approach involved the systematic examination of factors such as cell size, mesh size, the bed-load equation, and roughness height to discern their impact on simulation results.

5. IMPACT OF MESH SIZE, BED-LOAD EQUATION, AND ROUGHNESS HEIGHT

The study examined the impact of mesh size, bed-load equation, and roughness height concerning to both scenarios: one with rectangle debris situated 3 cm below the water surface and another without debris. Mesh size is crucial for model accuracy and can affect simulation duration. A mesh block with 300,000 cells was used, and higher resolution mesh planes were created around the pier to enhance accuracy (Fig. 8a and b).

Nielsen (N), Meyer Peter Müller (M), and Van Rijn (V) bed-load formulas have been utilized in the simulations and the outcomes were measured and compared with the results from the physical model. The results presented here demonstrate that the maximum scour estimates from V and M were 43% and 52%, respectively, lower than the N forecasts, where M predicts that V will be quite near the scouring depth. Nevertheless, the scouring and deposition patterns and morphologies produced by the V, and M equations are remarkably different. The N equation, which is combined with the RNG model to derive a more precise conclusion, is adequate in the bed-load effectiveness research

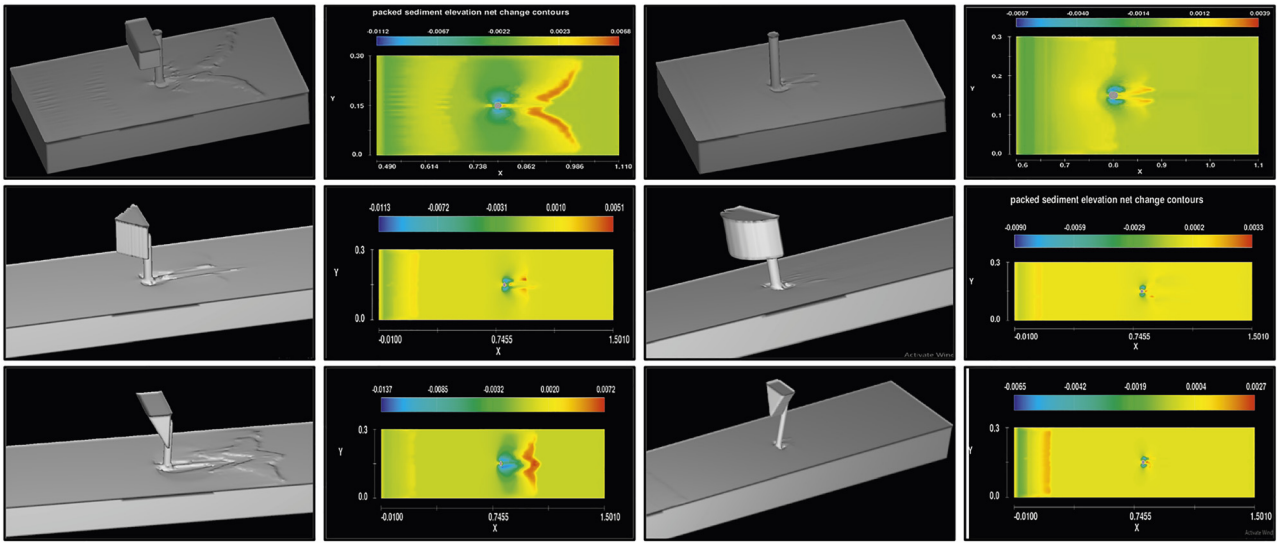

Fig. 7. The maximum scour depth of no-debris, rectangle, triangle bow, half-circle, high wedge, and triangle yield sign

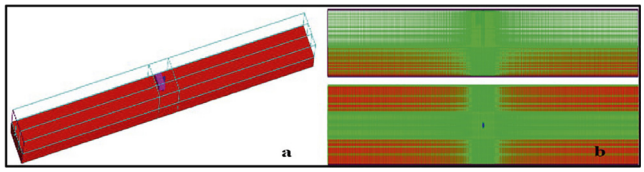

Fig. 8. a) Plan the meshing around the pier, b) plan, and side view of the model with meshing

in contrast to different simulation methods, which makes it remarkable. A roughness height is frequently estimated as a function of a typical grain size diameter; many researchers have focused on this parameter and concluded that the range value is 1–7 in D_{50}. These evaluations show that stating roughness level as an expression of grain size is fraught with uncertainty. To compare with the original parameter set value of $6 \times D_{50}$, it was examined the height values of 3 D_{50} and 6 D_{50} to comprehend the impact of this input. The undefined shear stress values that are calculated and used to drive the bed load and absorption algorithms are impacted directly by changes in factor multiplied by the sand diameter. The projected result of raising the roughness height will be an increase in bed stress due to shear force and scour levels.

As a result, several distinct types of mesh accuracy were used to get optimal calculation time values. Following several experiments to meet the phenomenon criteria, various cell sizes of 0.4, 0.3, and 0.2 cm were selected as the optimal cell size. Consequently, runs completed control the optimal mesh choice of 0.2 cm. When the roughness height is a default value of 2.5 D_{50} and employing Mayor as the transport equation with the mesh size of 0.3 cm, the anticipated numerical scour depth is underestimation by 65% in comparison with the experimental result of hydraulic conditions. Whereas if the roughness height increased to 6 D_{50} and Nilsen as bed load equation with the fine meshing of 0.2 cm size, the underestimation value would be 2% only with RMSE = 0.02 for no debris case as it can be seen in Figs 9 and 10 and 3% with RMSE = 0.03 when employed the rectangular debris with 3 cm below the water surface as it can be seen in Figs 11 and 12.

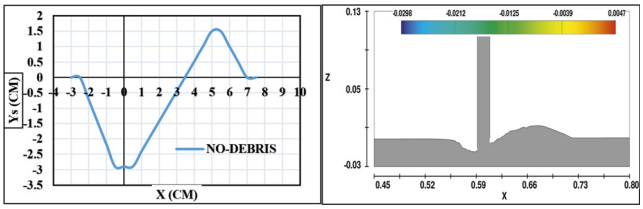

Fig. 9. The maximum scour depth of experimental vs. the numerical in *X-Z* direction for no debris case

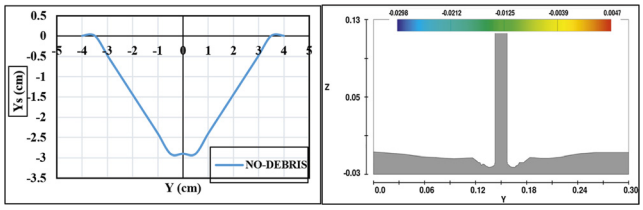

Fig. 10. The maximum scour depth of experimental vs. the numerical in *Y-Z* direction for no debris case

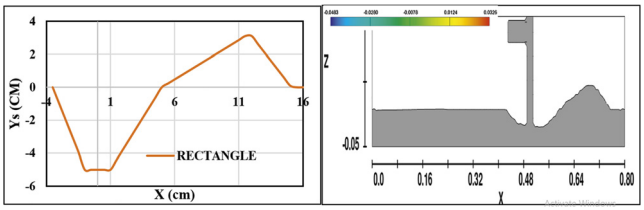

Fig. 11. The maximum scour depth of experimental vs. the numerical in *X-Z* direction for the rectangle debris at 3 cm below the water surface

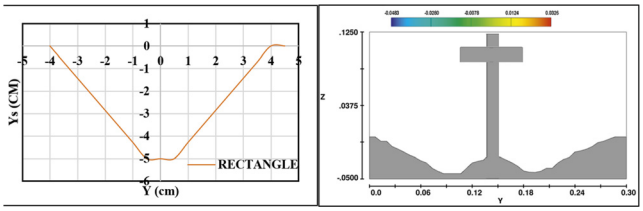

Fig. 12. The maximum scour depth of experimental vs. the numerical in *Y-Z* direction for the rectangle debris at 3 cm below the water surface

6. EMPIRICAL EQUATIONS FOR ENHANCED DEBRIS-AFFECTED SCOUR DEPTH

Several scour depth estimation equations have been selected to compare against the physical model results of this investigation. The empirical equations that received the most comments for calculating the scour depth are as follows:

- Melville and Y.M. Chiew (1999) [22];
- Richardson and S. R. Davies (2001) [23];
- D. M. Sheppard, B. Melville, and H. Demir (2014) [24].

Anticipated Eq. (1) from [25] to calculate the equivalent pier width as a consequence of the accumulation of debris,

$$De = \frac{T^* \cdot W \cdot D + \left(Y - T^*\right)D}{Y}, \qquad (1)$$

where De is the effective pier width (cm); T^* is the effective debris thickness, $0.52T$ (cm); W is the debris width (cm); D is the pier width (cm); Y is the flow depth (cm). To account for the scouring impact of debris, they advocated using an efficient pier width instead of the initial pier wide in neighborhood scouring calculations. The debris breadth and size, pier dimension, and elevation of the water in the stream are used to determine the effective diameter, which is greater compared to the real pier diameter (Table 1).

Following more studies in [26], Eq. (2) introduced the equivalent pier dimension method, a revised variant of the efficient pier dimension technique,

$$a = \frac{K_{d1} W \cdot T + (Y - K_{d1} T)D}{Y}, \qquad (2)$$

where K_{d1} is the coefficient as shape factor and is equal to 0.39 for rectangular debris and 0.14 for triangular debris in profile Table 2.

Once a computed effective width (De) is compared to an actual effective diameter, Eq. (1) overestimates the effective width of any pier if debris exists, especially in rectangular geometries. This equation ignores the form of the debris mass, as well as the length L of the debris reaching upstream from the pier.

Figure 13a and b compare the findings of this experimental research's single-pier scour depth measurement (Zs(MEAS.) with calculated scour depth (Zs(CAL) from the empirecal equations of [22, 23], and [24]. The findings of this study's experimental testing are described in Table 3.

7. EVALUATION OF SCOUR DEPTH PREDICTION METHODS IN THE PRESENCE OF DEBRIS

This study critically assesses two methods, one proposed by [25] and another by [26], for predicting scour depth around

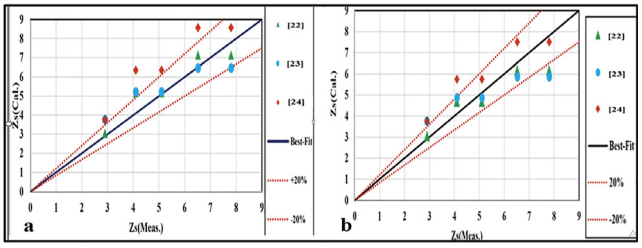

Fig. 13. a) Scour depth results of three estimation equations when applying Eq. (1) for calculating *De*, b)Scour depth results of three estimation equations when applying Eq. (2) for calculating *De*

Table 1. Effective pier width using Eq. (1) for the case of no-debris and rectangular debris

Case	W (cm)	L (cm)	T (cm)	Y (cm)	D (cm)	T^* (cm)	De (cm)
No-debris	–	–	–	12	2	–	2
Rectangular debris	12	6	3	12	2	1.56	3.30
	12	6	6	12	2	3.12	4.60
	12	12	3	12	2	1.56	3.30
	12	12	6	12	2	3.12	4.60

Table 2. Equivalent pier width using Eq. (2) for the case of no-debris and rectangular debris

Case	W (cm)	L (cm)	T (cm)	Y (cm)	D (cm)	a (cm)
No-debris	–	–	–	12	2	2
Rectangular debris	12	6	3	12	2	2.98
	12	6	6	12	2	3.95
	12	12	3	12	2	2.98
	12	12	6	12	2	3.95

Table 3. Empirical equations for evaluation debris-affected scour depth

The empirical equations	the *De* and a method	remarks
Reference [22]	Eq. (1)	Tends to mildly overestimate (RMSE = 0.8)
	Eq. (2)	Aligns closely with actual values (RMSE = 0.7)
Reference [23]	Eq. (1)	Incorporating initial debris length, yields improved estimates with RMSE = 0.86
	Eq. (2)	Tends to underestimation (RMSE = 1.13)
Reference [24]	Eq. (1)	Exhibits a propensity to overestimate scour depth (RMSE = 1.7)
	Eq. (2)	Improved estimates but still overestimation with RMSE = 0.99

bridge piers in the presence of debris. Despite some enhancements made to [26]'s method, both approaches share similar limitations and tend to overstate scour depth when compared to laboratory experiments, albeit to varying degrees. Notably, these methods are only effective when debris is slightly submerged below the flow-free level. However, this condition may not accurately represent the real-world scenario where obstructions and debris can be buried and found along the riverbed. In response to these shortcomings, this research introduces a novel equation to enhance scour depth prediction around bridge piers, taking into consideration various debris shapes, including rectangle, triangle bow, high wedge, low wedge, triangle yield sign, and half-cylinder. The investigation explores debris with different thicknesses, ranging from $T = 3$ cm (partially submerged) to $T = 12$ cm (fully submerged at the bottom of the flume). Building upon the findings of this study, which emphasized the significance of $L/D = 3$ for severe scour damage and maximum scour depth, this study also varies the length of debris between $L/D = 3$ and $L/D = 6$. Additionally, the debris's effective area ratio (A%) is considered, ranging from 3.1% to 33.3%. To derive the new equation, a series of multiple nonlinear regression analyses was conducted using the limited experimental data from this research. The resulting equation is expressed as:

$$Kd(\text{cal}) = 0.1174 \cdot (A\%) - 0.002 \cdot (A\%)^2 + 0.445 \cdot \left(\frac{L}{D}\right) - 0.0103 \cdot \left(\frac{L}{D}\right)^3. \quad (3)$$

The newly developed equation denoted as *Kd* proves to be a robust tool for predicting scour depth in the presence of debris when compared to the reference condition without debris (Kd(cal). In Fig. 14a and b this equation demonstrates a strong correlation with experimental data, boasting an R2 value of 81%, signifying a reliable relationship between predicted and observed values. The RMSE of 0.2 is remarkably low, considering the limitations of the dataset and the experimental nature of the data. An insightful analysis of residuals, calculated as the difference between measured scour depth (Kd (meas)) and predicted scour depth (Kd(cal), reveals an intriguing probabilistic distribution. The distribution curve displays a slight underestimation bias, with a slightly tilted, asymmetrical bell-shaped pattern. The highest likelihood of residuals centers around the average value, indicating that the predicted scour depths are generally close to the actual values. Importantly, the distribution curve never approaches zero likelihood, signifying that residuals never reach zero, even occasionally reaching as high as 0.2, suggesting a minor overestimation at times.

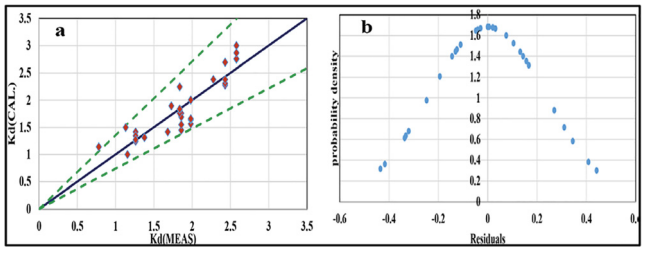

Fig. 14. a)The difference in calculation between the anticipated model Kd(cal) and physical model data Kd(MEAS), b) The probability density vs. residuals of the anticipated model

8. CONCLUSIONS

In this extensive study, the research aimed to investigate the impact of floating debris on local scour around bridge piers. The investigation combined experimental and numerical validation using the FLOW-3D software under consistent hydraulic conditions. This study, delved into the intriguing dynamics of hydraulic flow around a single pier and its interaction with various debris shapes. High wedge debris shapes induced significant scouring, profoundly impacting scour patterns, and flow.

It introduced a novel equation for predicting scour depth, which demonstrated a robust correlation with experimental data ($R_2 = 81\%$). This equation enhances our ability to forecast scour depths based on this experimental study data, providing valuable insights for real-world bridge scenarios. Further research can explore its practical applicability across diverse hydraulic conditions.

REFERENCES

[1] A. C. Parola, C. J. Apelt, and M. A. Jempson, *Debris Forces on Highway Bridges*. Washington, D.C.: National Academy Press, 2000.

[2] J. L. Briaud, H. C. Chen, Y. Li, P. Nurtjahyo, and J. Wang, "SRICOS-EFA method for contraction scour in fine-grained soils," *J. Geotech. Geoenvironmental Eng.*, vol. 131, no. 10, pp. 1283–1294, 2005.

[3] P. F. Lagasse and E. V. Richardson, "ASCE compendium of stream stability and bridge scour papers," *J. Hydraul. Eng.*, vol. 127, no. 7, pp. 531–533, 2001.

[4] P. Zampieri, M. A. Zanini, F. Faleschini, L. Hofer, and C. Pellegrino, "Failure analysis of masonry arch bridges subject to local pier scour," *Eng. Fail. Anal.*, vol. 79, pp. 371–384, 2017.

[5] M. Ebrahimi, P. Kripakaran, D. Prodanović, R. Kahraman, M. Riella, G. Tabor, and S. Djordjević, "Experimental study on scour at a sharp-nose bridge pier with debris blockage," *J. Hydraul. Eng.*, vol. 144, 2018, Art no. 4018071.

[6] S. Pagliara and I. Carnacina, "Influence of large woody debris on sediment scour at bridge piers," *Int. J. Sediment. Res.*, vol. 26, no. 2, pp. 121–136, 2011.

[7] E. Rahimi, K. Qaderi, M. Rahimpour, M. M. Ahmadi, and M. R. Madadi, "Scour at side by side pier and abutment with debris accumulation," *Mar. Georesources Geotechnol.*, vol. 39, no. 4, pp. 459–470, 2021.

[8] S. Das, R. Das, and A. Mazumdar, "Circulation characteristics of horseshoe vortex in scour region around circular piers," *Water Sci. Eng.*, vol. 6, no. 1, pp. 59–77, 2013.

[9] S. Y. Lim, "Equilibrium clear-water scour around an abutment," *J. Hydraul. Eng.*, vol. 123, no. 3, pp. 237–243, 1997.

[10] Y. M. Chiew, "Local scour and riprap stability at bridge piers in a degrading channel," *J. Hydraul. Eng.*, vol. 130, no. 3, pp. 218–226, 2004.

[11] B. E. Hunt, *Monitoring Scour Critical Bridges*. Transportation Research Board, 2009.

[12] E. V Richardson and S. R. Davis, "Evaluating scour at bridges," United States. Federal Highway Administration. Office of Technology Applications, 1995.

[13] M. Al-Jubouri and R. P. Ray, "A comparative study of local scour depth around bridge piers," *Pollack Period.*, vol. 18, no. 1, pp. 100–105, 2023.

[14] M. Spasojevic and F. M. Holly Jr., "Two-and three-dimensional numerical simulation of mobile-bed hydrodynamics and sedimentation," *Sediment. Eng. Process. Meas. Model. Pract.*, pp. 683–761, 2008.

[15] B. W. Melville, "Pier and abutment scour: an integrated approach," *J. Hydraul. Eng.*, vol. 123, no. 2, pp. 125–136, 1997.

[16] B. W. Melville and S. E. Coleman, *Bridge Scour*. Water Resources Publication, 2000.

[17] A. Khosronejad, C. Hill, S. Kang, and F. Sotiropoulos, "Computational and experimental investigation of scour past laboratory models of stream restoration rock structures," *Adv. Water Resour.*, vol. 54, pp. 191–207, 2013.

[18] A. Kumar, U. C. Kothyari, and K. G. R. Raju, "Flow structure and scour around circular compound bridge piers - A review," *J. Hydro-environment Res.*, vol. 6, no. 4, pp. 251–265, 2012.

[19] L. Tugyi, Z. Siménfalvi, G. L. Szepesi, C. Kecskés, Z. Kerekes, and T. Sári, "CFD modeling of subsonic and sonic methane gas release and dispersion," *Pollack Period.*, vol. 18, no. 3, pp. 99–105, 2023.

[20] I. S. P. Mendonça, H. D. L. Canilho, and C. M. S. Fael, "Flow-3D modeling of the debris effect on maximum scour hole depth at bridge piers," in *38th IAHR World Congress*, Panama City, Panama, September 1–6, 2019, pp. 2813–2821.

[21] M. A. Sarker, "Flow measurement around scoured bridge piers using Acoustic-Doppler Velocimeter (ADV)," *Flow Meas. Instrum.*, vol. 9, no. 4, pp. 217–227, 1998.

[22] B. W. Melville and Y. M. Chiew, "Time scale for local scour at bridge piers," *J. Hydraul. Eng.*, vol. 125, no. 1, pp. 59–65, 1999.

[23] E. V. Richardson and S. R. Davies, "Evaluating scour at bridge pier," Report no. FHWA HIF-12-003, U.S. Department of Transportation, Federal Highway Administration, pp. 1–340, 2002.

[24] D. M. Sheppard, B. Melville, and H. Demir, "Evaluation of existing equations for local scour at bridge piers," *J. Hydraul. Eng.*, vol. 140, no. 1, pp. 14–23, 2014.

[25] B. W. Melville and D. M. Dongol, "Bridge pier scour with debris accumulation," *J. Hydraul. Eng.*, vol. 118, no. 9, pp. 1306–1310, 1992.

[26] P. F. Lagasse, L. W. Zevenbergen, and P. E. Clopper, "Impacts of debris on bridge pier scour," in *Proceedings 5th International Conference on Scour and Erosion*, San Francisco, USA, November 7–10, 2010, pp. 854–863.